

## Enhanced Adsorption of Molecules on Surfaces of Nanocrystalline Particles

Hengzhong Zhang,<sup>†</sup> R. Lee Penn,<sup>†</sup> Robert J. Hamers,<sup>‡</sup> and Jillian F. Banfield<sup>\*,†</sup>

Department of Geology and Geophysics and Department of Chemistry, University of Wisconsin—Madison, Madison, Wisconsin 53706

Received: December 2, 1998; In Final Form: April 5, 1999

Quantitative measurements of adsorption from solution show up to a 70-fold increase in the adsorption coefficient when a variety of organic acids are adsorbed onto 6 nm compared to 16 nm nanocrystalline titania particles. A Langmuir adsorption model modified to include the dependence of interfacial tension (interfacial free energy) on particle size predicts an increase in the adsorption constant ( $K_{\text{ads}}$ ) as the crystallite size decreases, in agreement with the experimental results. The increase in  $K_{\text{ads}}$  arises predominantly from the increased molar surface free energy of the nanocrystalline particles. The rapid increase in adsorption as particle size decreases has important implications for understanding and modeling natural and experimental systems.

### Introduction

Adsorption of ions and molecules on the surfaces of solid particles is a critical step in crystal growth, surface catalysis, and many other physical and chemical phenomena.<sup>1</sup> As the dimensions of the particles shrink into the nanometer range, there are significant changes in optical and electronic properties due both to quantum size effects and to the increasingly important role of the surface in controlling the overall energy of the particles.<sup>2</sup> While many of the unusual physical properties of these nanocrystalline materials are now well understood, the influence of size on the chemical properties, such as adsorption coefficients and chemical reactivity, remains poorly understood. Stark et al. studied the adsorption of gaseous SO<sub>2</sub>, CO<sub>2</sub>, HCl, HBr, NO, and SO<sub>3</sub> onto the surfaces of nanoscale and micrometer-sized MgO particles.<sup>3</sup> It was found that at higher gas partial pressures, physical adsorption dominates and the micrometer-sized MgO adsorbed more molecules of a gas per unit surface area than nanoscale MgO because multilayers of gases can form more easily on flat surfaces than on curved surfaces. However, at lower gas partial pressures, monolayer chemical adsorption dominates and the nanoscale MgO adsorbed more gases than the micrometer-sized MgO. The heats of adsorption of cyclohexane on ultrafine MgO were determined by calorimetry.<sup>4</sup> It was found that the adsorption is a surface chemical adsorption and that the heat of the adsorption per unit area of MgO increases with a decrease in MgO size, which also suggests that finer MgO powders can adsorb more quantities of cyclohexane. Mentioned in the report of Vayssieres et al.<sup>5</sup> was that, in an aqueous solution, finer nanocrystalline magnetite particles have higher surface charge densities than larger ones. In these studies, the adsorbates were molecules that are of regular sizes or ions in a solution. Under these circumstances we will show that the influence of particle size on adsorption equilibrium can be treated quantitatively by using a thermodynamic approach. However, as the dimension of the adsorbate becomes larger, especially when it is comparable to the size of nanocrystalline particles, steric interactions among molecules

and/or between molecules and nanocrystalline particles may also become size-dependent because of the surface curvature. The concept of the mean free path of the Brownian motion of ultrafine hematite particles was used by Furusawa et al.<sup>6</sup> to explain their experimental observation that the maximum adsorption of polymers on the nanocrystalline hematite particles (mg g<sup>-1</sup>) increases with decreasing particle radius. Katari et al.<sup>7</sup> reported that total ligand saturation on nanocrystal CdSe surfaces varied from 60% for smaller nanocrystals to 30% in larger nanocrystals, which was attributed to steric considerations. To the contrary, Luzinov et al.<sup>8</sup> observed that the saturation adsorption of a polymer per unit surface area decreased as the adsorbent particles decreased in size. However, in their experiments the adsorbents of different sizes were of different chemical composition; this then clouds the issue of whether the observed effects can be attributed to chemical or size effects.

Although some insights of the size effect on the adsorption of molecules onto nanocrystalline particles were presented, a reasonable theoretical description and more straightforward experimental verification of the size effect on adsorption are necessary to further our understanding of the physical chemical nature of the effect. In this paper, we will present both our thermodynamic analysis and experimental determination of the influence of particle size on the adsorption of molecules from a solution onto nanocrystalline particles.

### Thermodynamic Analysis

The thermodynamic driving force for adsorption at a surface is typically described using the concept of free energy. The overall free energy change for adsorption from solution onto a surface is a function of the chemical composition and structure of the solid, as well as the nature of the solution. For a fixed set of solution parameters, however, the influence of particle size on the adsorption can be described thermodynamically by an equilibrium adsorption constant ( $K_{\text{ads}}$ ), also termed adsorption coefficient, which can be determined experimentally by measuring the extent of surface adsorption as a function of solution concentration.

Nanocrystalline materials fall into a regime where classical thermodynamics begins to overlap with atomistic lattice-based theories for understanding physical and chemical behavior. The

\* To whom correspondence should be addressed. E-mail: jill@geology.wisc.edu.

<sup>†</sup> Department of Geology and Geophysics.

<sup>‡</sup> Department of Chemistry.

relationship among  $K_{\text{ads}}$ , surface free energy, and crystal size can be defined using a classical thermodynamic approach. To understand how the particle size influences adsorption onto the particle surfaces, we use a simple Langmuir-type adsorption isotherm. In the Langmuir isotherm, the probability of a molecule adsorbing at any surface location is independent of the total surface coverage and dependent only on whether the specific adsorption site is already occupied or not.<sup>9</sup> For particles of a given size, the Langmuir isotherm is

$$\Gamma = \Gamma_{\text{max}} \frac{K_{\text{ads}}[\text{I}]}{1 + K_{\text{ads}}[\text{I}]} \quad (1)$$

where  $[\text{I}]$  presents the activity, i.e., the effective concentration of the adsorbate in the solution,  $\Gamma$  is the number of molecules adsorbed per unit surface area, and  $\Gamma_{\text{max}}$  is the maximum number of molecules per unit area that can be adsorbed.  $\Gamma_{\text{max}}$  is limited by the number of available surface sites.  $K_{\text{ads}}$  can be calculated thermodynamically, using

$$K_{\text{ads}} = \exp\left(-\frac{\Delta G_{\text{ads}}^{\circ}}{RT}\right) \quad (2)$$

where  $\Delta G_{\text{ads}}^{\circ}$  is the free energy change for the adsorption reaction,  $R$  is the universal gas constant ( $8.314 \text{ J mol}^{-1} \text{ K}^{-1}$ ), and  $T$  is the absolute temperature. If we evaluate the ratio of  $K_{\text{ads}}$  for two particles A and B of different size (radius  $r_{\text{A}} < \text{radius } r_{\text{B}}$ ), we find

$$\begin{aligned} \frac{K_{\text{ads}}(\text{A})}{K_{\text{ads}}(\text{B})} &= \exp\left(-\frac{\Delta G_{\text{ads}}^{\circ}(\text{A}) - \Delta G_{\text{ads}}^{\circ}(\text{B})}{RT}\right) \\ &= \exp\left(-\frac{[G_{\text{S-I}}^{\circ}(\text{A}) - G_{\text{S-I}}^{\circ}(\text{B})] - [G_{\text{S}}^{\circ}(\text{A}) - G_{\text{S}}^{\circ}(\text{B})]}{RT}\right) \end{aligned} \quad (3)$$

In eq 3,  $G_{\text{S-I}}^{\circ}$  and  $G_{\text{S}}^{\circ}$  represent the standard free energy of the adsorbate–surface site complex (S–I) and the surface site (S), respectively. The difference between  $G_{\text{S-I}}^{\circ}(\text{A})$  and  $G_{\text{S-I}}^{\circ}(\text{B})$  [or between  $G_{\text{S}}^{\circ}(\text{A})$  and  $G_{\text{S}}^{\circ}(\text{B})$ ] is caused only by the difference in particle size. Conventionally, the free energy difference can be calculated as follows.

At constant temperature and standard pressure,

$$\Delta G^{\circ} = \int_{r=\infty}^r \gamma_0 \, dA$$

where  $A$  stands for the molar surface area of the particles and  $\gamma_0$  the interfacial tension (interfacial free energy per unit area) between the solution and the particle, which is considered to be independent of curvature. So,  $\gamma_0$  virtually represents the interfacial tension between a flat surface and a solution. For spherical particles, the molar surface area  $A = 3V_{\text{m}}/r$  where  $V_{\text{m}}$  is the molar volume of the particle (see eq11). Combining these relationship with eq 3, we get

$$\frac{K_{\text{ads}}(\text{A})}{K_{\text{ads}}(\text{B})} = \exp\left\{-\frac{3V_{\text{m}}[\gamma_{0(\text{S-I})} - \gamma_{0(\text{S})}]}{RT} \left[\frac{1}{r_{\text{A}}} - \frac{1}{r_{\text{B}}}\right]\right\} \quad (4)$$

where the molar volume of the particle before and after adsorbing species I is considered the same;  $\gamma_{0(\text{S-I})}$  and  $\gamma_{0(\text{S})}$  represent, respectively, the interfacial tension of macroscopic

particles with and without adsorbing species I from the solution. According to the generalized Gibbs equation,

$$d\gamma = -\sum \Gamma_i d\mu_i \quad (5)$$

when adsorption occurs, i.e., positive adsorption is attained ( $\Gamma > 0$ ) when the chemical potential  $\mu_i$  of a species I increases, interfacial tension always decreases. Thus,  $\gamma_{0(\text{S-I})} - \gamma_{0(\text{S})} < 0$ . As a result,  $K_{\text{ads}}(\text{A}) > K_{\text{ads}}(\text{B})$ , in accordance with eq 4.

The above consideration does not take into account the influence of size on the interfacial tension itself. Experimental results have shown a size-related excess grain boundary energy of ultrafine-grained titania samples.<sup>10</sup> The enthalpy change of the tetragonal-cubic transformation of  $\text{BaTiO}_3$  was found to decrease with a decrease in particle size.<sup>11</sup> Recent experimental results have clearly demonstrated a decrease of grain boundary enthalpy of nanocrystalline selenium with the decrease of the selenium grain size.<sup>12</sup> These experimental observations strongly suggest that surface or interfacial tension of nanocrystalline particles can be modified significantly by the size of the particles. For liquid droplets, Tolman derived an equation describing the influence of droplet size on surface tension.<sup>13</sup> Equilibrium between the liquid droplet and its vapor was assumed in the derivation, which makes direct application of the result of the Tolman treatment to ultrafine solid particles (such as isolated fine particles) inappropriate. In this work, we employ a more direct and self-consistent approach to treat the particle size dependence of surface or interfacial tension of fine solid particles by making use of Maxwell's relationship of the second law of thermodynamics.<sup>14</sup>

For solids, while the properties of the bulk materials are uniform, this uniformity is interrupted at the surface of the solids. Coordination numbers, bond lengths, and bond angles of atoms on the first several layers of atoms on the solid surface are distinctly different from those of the bulk atoms. Thus, physical chemical quantities (such as the average energy) associated with the surface atoms are different from those of interior atoms. A simple physical picture of this structure is to treat a solid particle thermodynamically to be composed of two "phases": the surface phase consisting of atoms on or near the surface with a thickness of  $\delta$ , and the bulk phase consisting of the rest of the atoms (bulk atoms). Approximately, the surface phase can be viewed as having a thickness of one to several atom layers.

Consider 1 mol of spherical solid particles (radius  $r$ ) immersed in a solution. We assume that the particles are insoluble, incompressible, and isotropic. According to thermodynamic principle, the following equation applies for the system consisting of the 1 mol of the solid particles and their nearby solution.

$$dG = -S \, dT + V \, dP + \sum \mu_i \, dn_i + \gamma \, dA \quad (6)$$

where  $P$  represents the pressure,  $G$ ,  $S$ , and  $V$  are Gibbs free energy, entropy, and volume of the system, respectively, and  $n_i$  is the molar number of species  $i$  in the solution. Here, the interfacial tension  $\gamma$  is considered as a function of particle size at constant temperature and ambient pressure ( $P_0$ ). According to the Laplace equation,<sup>15</sup> atoms on the surface of a solid particle exert an excess pressure ( $P_{\text{exc}}$ ) on the bulk atoms of the particle

$$P_{\text{exc}} = \frac{2\sigma}{r} \quad (7)$$

where  $\sigma$  is the surface stress of the particle. First-principle calculations revealed that the surface stress of metals is about 1–2 times the surface tension in value.<sup>16</sup> If the surface stress

of a material is close to its surface tension in value, it means that the average energy of the surface atoms is less affected by the surface strain, or the surface strain is nearly zero. Empirically, we can express their relationship as  $\sigma = t\gamma$  where  $t$  is a multiplicative factor. For titania, the assumption that the surface stress equals the surface tension in value (i.e.,  $t = 1$ ) resulted in good agreement between the thermodynamic prediction and the experimental observation for the phase stability of nanocrystalline titania.<sup>17</sup> If the relative magnitude of the surface stress and the surface tension is unknown,  $t = 1$  can be regarded as a reasonable approximation. Now, eq 6 can further be written as

$$dG = -S dT + (V - V_{\text{bulk}}) dP_0 + V_{\text{bulk}} d(P_0 + P_{\text{exc}}) + \sum \mu_i dn_i + \gamma dA \quad (8)$$

where  $V_{\text{bulk}}$  represents the total volume of the bulk phase of all the particles involved. At constant temperature and ambient pressure, eq 8 reduces to

$$dG = V_{\text{bulk}} dP_{\text{exc}} + \sum \mu_i dn_i + \gamma dA \quad (9)$$

The number of particles ( $n$ ) can be calculated from the molar volume  $V_m$

$$n = \frac{V_m}{(4/3)\pi r^3} \quad (10)$$

and thus,  $A$  and  $V_{\text{bulk}}$  are, respectively,

$$\begin{aligned} A &= 4\pi r^2 n \\ &= \frac{3V_m}{r} \end{aligned} \quad (11)$$

and

$$\begin{aligned} V_{\text{bulk}} &= \frac{4}{3}\pi(r - \delta)^3 n \\ &= V_m \left(1 - \frac{\delta}{r}\right)^3 \end{aligned} \quad (12)$$

Applying Maxwell relation in eq 9,

$$\left(\frac{\partial \gamma}{\partial P_{\text{exc}}}\right) = \left(\frac{\partial V_{\text{bulk}}}{\partial A}\right) \quad (13)$$

Inserting eqs 7, 11, and 12 into eq 13 and noting that only  $r$  is an independent variable, we obtain

$$\frac{d \ln \gamma}{dr} = \frac{2t \left(1 - \frac{\delta}{r}\right)^2 \left(\frac{\delta}{r}\right) \frac{1}{r}}{1 + 2t \left(1 - \frac{\delta}{r}\right)^2 \left(\frac{\delta}{r}\right)} \quad (14)$$

Integration of above equation yields

$$\begin{aligned} \ln\left(\frac{\gamma}{\gamma_0}\right) &= -\int_0^{\delta/r} \frac{2t(1-x)^2}{1 + 2t(1-x)^2 x} dx \\ &= -\int_0^{\delta/r} F(x) dx \end{aligned} \quad (15)$$

where the function  $F(x)$  represents the corresponding part in eq 15. Figure 1 (at  $t = 1$ ) shows that the interfacial tension

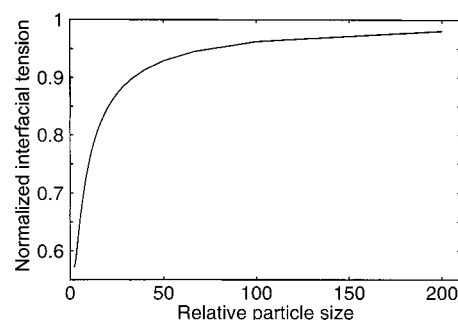


**Figure 1.** Decrease of interfacial tension with particle size. Relative particle size equals particle size divided by surface thickness ( $r/\delta$ ), which is dimensionless. Normalized interfacial tension is  $\gamma/\gamma_0$ .

decreases markedly as the particle size approaches the dimension of the thickness of the surface phase. Physically, the decrease in interfacial tension with decreasing particle size can be interpreted as mainly due to the increase in the potential energy ( $V_{\text{bulk}} dP_{\text{exc}}$ ) of the bulk atoms as a result of the excess pressure the bulk attained.

We now calculate the free energy change of the system caused only by the change in particle size. Inserting  $\gamma$  from eq 15 into eqs 7 and 9 and inserting eqs 11 and 12 and the resulting eq 7 into eq 9, a differential equation relating the free energy change with the particle radius is generated. Integrating the differential equation from infinite particle size to radius  $r$ , we obtain

$$\begin{aligned} \Delta G &= G(\text{radius } r) - G(\text{radius } \infty) \\ &= \frac{2tV_m\gamma_0}{\delta} \Phi\left(\frac{\delta}{r}\right) + \frac{3V_m\gamma_0}{\delta} \Theta\left(\frac{\delta}{r}\right) \end{aligned} \quad (16)$$

where the functions

$$\Phi(x) = \int_0^x \frac{(1-x)^3 \exp(-\int_0^x F(x) dx)}{1 + 2t(1-x)^2 x} dx \quad (17)$$

$$\Theta(x) = \int_0^x \exp(-\int_0^x F(x) dx) dx \quad (18)$$

Numerically, eq 16 can be represented as a regression equation:

$$\Delta G = \frac{V_m\gamma_0}{r} f\left(\frac{\delta}{r}\right) \quad (19)$$

where  $f(\delta/r)$  is a regression function (eq 20) with  $\delta/r$  as its variable (at  $t = 1$ ):

$$f(x) = 5.00 - 7.52x + 8.11x^2 - 3.29x^3 \quad (0 < x < 1) \quad (20)$$

A plot (not shown) of  $\Delta G$  versus the particle radius at a fixed surface thickness shows a dramatic increase in the free energy of the system when the particle size decreases. This can be understood by noting that the surface stress creates an internal pressure that exceeds the external pressure and that increases the potential energy of the bulk, as well as the molar surface area increases, which increases the free energy of the surface. Therefore, there is an increase in the molar free energy for small particles compared with larger ones. Thus, for example, small-diameter solids are known to have higher vapor pressures and lower melting points than their macroscopic counterparts. Under such considerations, when eq 19 is inserted into eq 3, the ratio

of  $K_{\text{ads}}$  for the two particles A and B becomes

$$\frac{K_{\text{ads}}(\text{A})}{K_{\text{ads}}(\text{B})} = \exp \left\{ - \frac{V_{\text{m}}[\gamma_{0(\text{S}-1)} - \gamma_{0(\text{S})}]}{RT} \left[ \frac{1}{r_{\text{A}}} f\left(\frac{\delta}{r_{\text{A}}}\right) - \frac{1}{r_{\text{B}}} f\left(\frac{\delta}{r_{\text{B}}}\right) \right] \right\} \quad (21)$$

Since the function  $f(\delta/r)/r$  decreases monotonically with increased particle size,  $K_{\text{ads}}(\text{A}) > K_{\text{ads}}(\text{B})$  according to eq 21.

Both eqs 4 and 21 predict that the adsorption constant increases at small particle sizes. This conclusion is reasonable because a reduction of total free energy is an important driving force for adsorption, so finer particles with increased energy should be more prone to adsorb molecules onto their surfaces. However, the extent to which the adsorption constant can increase as particle size decreases is different when it is calculated from eq 4 and from eq 21. Or, if the extent is the same, the model parameters used by eqs 4 and 21, such as the interfacial tension at infinite size,  $\gamma_{0(\text{S}-1)}$ , can be quite different. This may be used to justify which equation (eq 21 or eq 4) is more reasonable.

## Experimental Section

To test the thermodynamic model presented above and to directly and explicitly examine the particle size effect on adsorption, we measured the adsorption of acetic, valeric, oxalic, and adipic acids onto the surfaces of titania particles having different sizes (average diameters of 6 and 16 nm) in aqueous solutions at room temperature. Anatase particles ( $\text{TiO}_2$ , anatase phase) were prepared by the sol-gel route.<sup>18</sup> The size and shape of these particles were measured directly via transmission electron microscopy (TEM) and by X-ray diffraction (XRD) peak-broadening analysis. Peak-broadening analysis measures diffraction from a large number of nanocrystals simultaneously, yielding an average crystal size of 6 nm for the material. TEM data show the particles are equidimensional, and so the surface area was determined using a spherical approximation. The calculated surface area of  $260 \text{ m}^2 \text{ g}^{-1}$  is almost exactly consistent with numerical interpolation of the BET surface area measurements of nanocrystalline titania prepared using the same method.<sup>19</sup> Larger particles were prepared by coarsening the 6 nm particles under hydrothermal conditions.<sup>20</sup> Particle diameters were measured along  $\{001\}$  and  $\{101\}$  by XRD peak-broadening analysis, and surface areas were calculated using the particle shape determined by TEM. The surface area calculated for the 16 nm diameter particles is  $80 \text{ m}^2 \text{ g}^{-1}$ , which is appropriately larger than the area of a sphere of the same diameter due to the presence of significant faceting, dominated by  $\{101\}$  and  $\{001\}$  planes.

The total amount of surface adsorption (per unit surface area) was determined by using high-pressure liquid chromatography (Shimadzu HPLC) to measure the concentration of analytes remaining in solution. The adsorption amount was determined as a function of solution concentration. Solutions of acetic, valeric, adipic, and oxalic acids with concentrations up to 0.08 M concentration were used. Since the solutions were not buffered, the pH values varied with the acid concentration. Acetic ( $\text{p}K_{\text{a}} = 4.81$ ) and valeric ( $\text{p}K_{\text{a}} = 4.76$ ) acids are monocarboxylic, while adipic ( $\text{p}K_{\text{a},1} = 4.43$ ,  $\text{p}K_{\text{a},2} = 5.41$ ) and oxalic ( $\text{p}K_{\text{a},1} = 1.27$ ,  $\text{p}K_{\text{a},2} = 4.28$ ) acids are dicarboxylic. Figure 2 shows the calculated speciation and solution pH as a function of acid concentration. For acetic, valeric, and adipic acids the fully protonated forms dominate in solution; for oxalic acid both the fully protonated and single-deprotonated forms are significant.

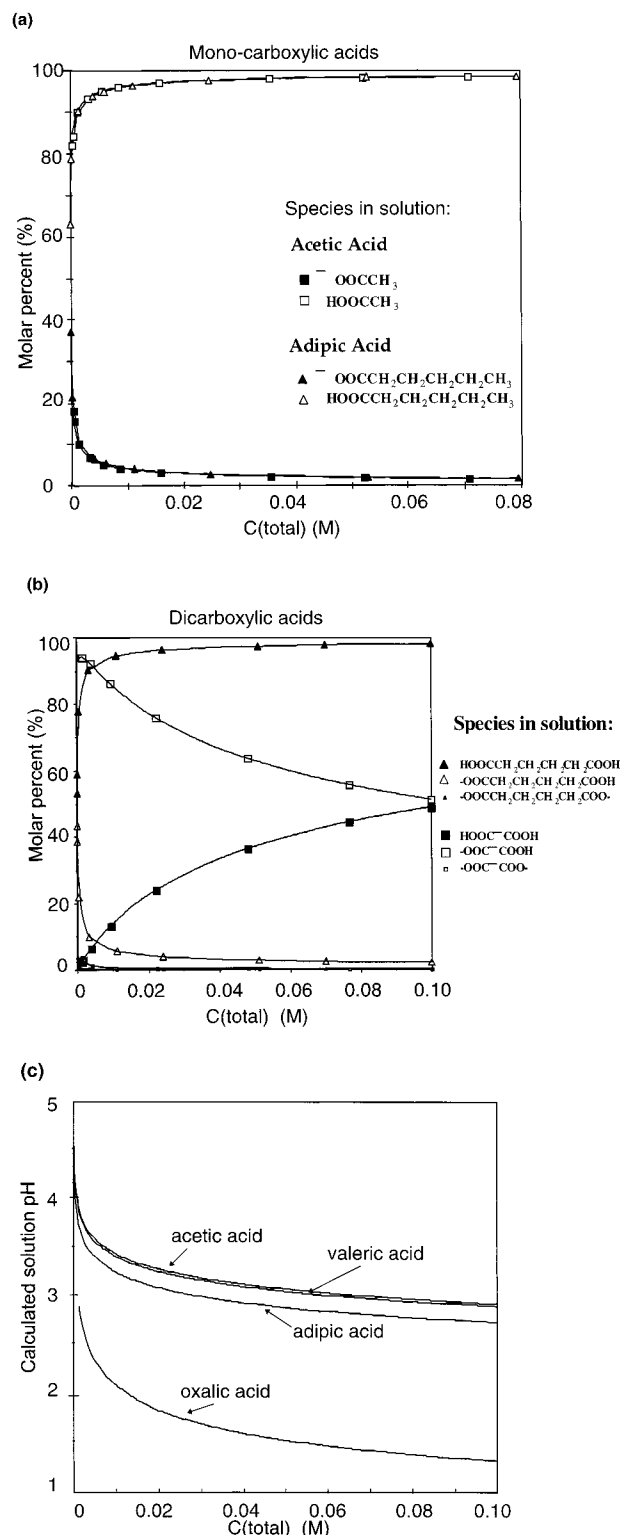


**Figure 2.** Distribution of species in solution for (a) acetic acid ( $\text{CH}_3\text{-COOH}$ ) and valeric acid [ $\text{CH}_3(\text{CH}_2)_4\text{COOH}$ ], (b) adipic acid [ $\text{HOOC}(\text{CH}_2)_4\text{COOH}$ ] and oxalic acid ( $\text{HOOC-COOH}$ ). (c) Variation of solution pH with the total concentration.

## Results and Discussion

Figure 3 shows the amount of surface adsorption as a function of equilibrium concentration for acetic, oxalic, valeric, and adipic acids on both 6 and 16 nm diameter particles, along with fits to a Langmuir adsorption isotherm (eq 1) as described in more detail below. Table 1 shows the numerical values of the results from the fit. Several features in Figure 3 are immediately



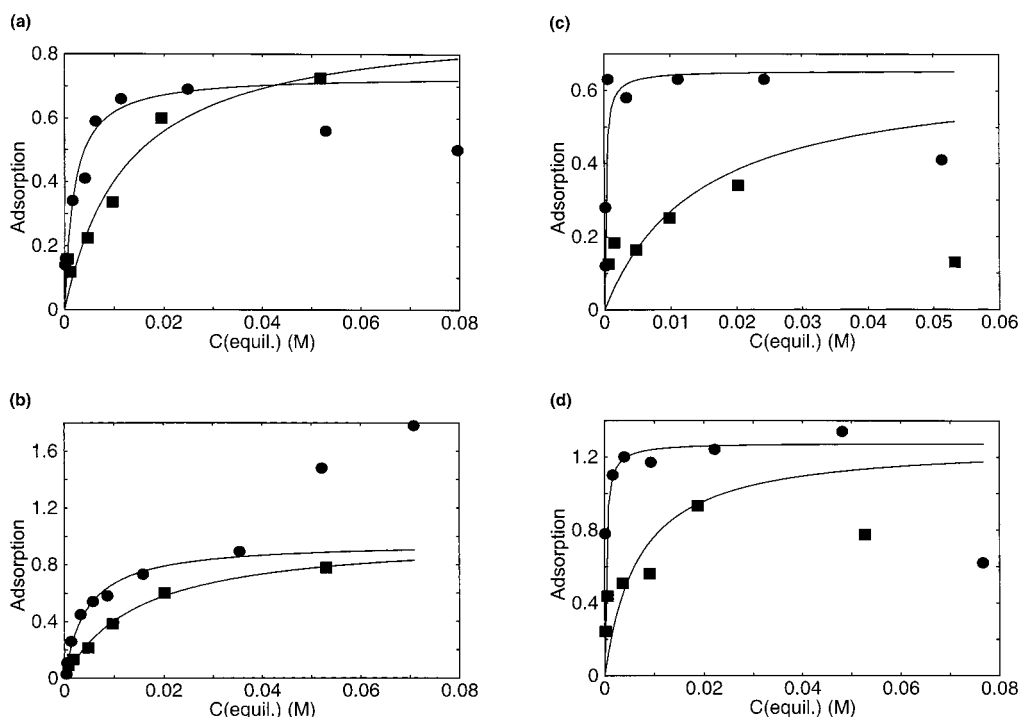


**Figure 3.** Adsorption (molecules nm<sup>-2</sup>) of (a) valeric, (b) acetic, (c) adipic, and (d) oxalic acids onto 6 nm (circular points) and 16 nm (square points) diameter anatase particles. Lines are the fitting with Langmuir adsorption isotherm.

**TABLE 1: Modeling Results for Data (Shown in Figure 3) of Adsorption of Organic Acids on Nanocrystalline Titania Particles of Different Sizes**

adsorbate (acid)	$K_{\text{ads}}(6 \text{ nm})$ (mol <sup>-1</sup> )	$K_{\text{ads}}(16 \text{ nm})$ (mol <sup>-1</sup> )	$\Gamma_{\text{max}}(6 \text{ nm})$ (mol nm <sup>-2</sup> )	$\Gamma_{\text{max}}(16 \text{ nm})$ (mol nm <sup>-2</sup> )	$K_{\text{ads}}(6 \text{ nm})/$ $K_{\text{ads}}(16 \text{ nm})$
valeric	530.6	78.6	0.74	0.91	6.8
acetic	227.8	67.9	0.96	1.00	3.4
adipic	4890.0	70.0	0.65	0.65	69.9
oxalic	3510.0	149.3	1.28	1.28	23.5

apparent. First, we note that at low concentrations the plots for 6 nm particles have a significantly steeper slope than those for 16 nm particles, for all four acids. Since in the Langmuir adsorption isotherm the plot of surface coverage vs concentration has a slope at infinite dilute concentration equal to the equilibrium constant  $K_{\text{ads}}$ , this in turn indicates that the small particles have significantly larger equilibrium constants for adsorption on the surface, in agreement with the thermodynamic analysis presented above.

A second feature in Figure 3 is that for oxalic, adipic, and valeric acids at higher concentrations,  $\Gamma$  decreases to less than  $\Gamma_{\text{max}}$ . According to the Langmuir model, adsorption should increase monotonically to a limiting value  $\Gamma_{\text{max}}$ , while Figure 3 reveals somewhat more complex behavior that may have several origins. We attribute the decreases in surface adsorption at high concentration to activity effects, which cause the effective concentrations of species in solution to be lower than their physical concentrations. In contrast, acetic acid exhibits a second rapid increase as the concentration is increased beyond about 0.04 M. The source of this may be multilayer formation.

While the strong deviations from ideal behavior at high solution concentrations are expected to lead to a failure of simple adsorption models, in the low-concentration region where solutions behave more ideally a Langmuir-type isotherm may still yield useful information. For this reason, Figure 3 also shows fits of the experimental data in the low-concentration region ( $<0.05 \text{ M}$ ) to a Langmuir isotherm. As expected, the fits for each acid show a strong influence of nanocrystal size on the equilibrium constant. The effect of size on  $\Gamma_{\text{max}}$  is difficult

to interpret because of a variety of competing effects, including relative sizes of molecules and adsorbents and changes in activity coefficients and pH with increasing solution concentration. However, the results in Table 1 show that for valeric and acetic acids the  $\Gamma_{\text{max}}$  is almost unaffected by crystal size. This is an important result because it shows that the enhanced adsorption on the small nanocrystals cannot be due to an error in surface area measurement but must be a true change in equilibrium constant. For adipic and oxalic acids a value of  $\Gamma_{\text{max}}$  cannot be derived from the experimental data because the adsorption has not reached its maximum value before it is suppressed by a change in the activity coefficient. On the basis of the behavior of acetic and valeric acids, we assume that  $\Gamma_{\text{max}}$  for adsorption of adipic and oxalic acids onto 16 nm particles is similar to that onto 6 nm particles. Fitting of experimental data allows determination of  $K_{\text{ads}}$  for all oxalic and adipic acids on 16 nm particles, as shown in Table 1.

The experimental values shown in Table 1 can be compared with the values predicted by eq 21 if the variables in this equation are known. Although precise values of all parameters are not available, reasonable estimates can be made. For anatase, the bulk molar volume of  $V_{\text{m}} = 2.05 \times 10^{-5} \text{ m}^3 \text{ mol}^{-1}$  can be used,<sup>21</sup> as well as the interfacial tension of  $\gamma_{\text{O(S)}} = 1.0 \text{ J m}^{-2}$ .<sup>22</sup> The surface layer thickness  $\delta$  should be on the order of the atomic lattice spacing; we thus take  $\delta = 0.35 \text{ nm}$  [lattice parameter of (101) anatase]. In order for the experimentally measured  $K_{\text{ads}}(6 \text{ nm})/K_{\text{ads}}(16 \text{ nm})$  and theoretically predicted values for  $K_{\text{ads}}(6 \text{ nm})/K_{\text{ads}}(16 \text{ nm})$  to agree, the value for  $\gamma_{\text{O(S-I)}}$  is  $0.72 \text{ J m}^{-2}$  for valeric acid,  $0.82 \text{ J m}^{-2}$  for acetic acid,  $0.38$

$\text{J m}^{-2}$  for adipic acid, and  $0.54 \text{ J m}^{-2}$  for oxalic acid. These results imply that adsorption of the larger molecules depresses the interfacial tension more than adsorption of smaller molecules. We note that at solution–air interfaces the efficacy of long-chain hydrocarbons such as soaps (typically long-chain alkyl sulfonates) for decreasing the surface tension also scales with the length of the hydrocarbon chain. For both the solution–air and solution–solid interfaces, reduction in surface tension is related to the elimination of polar bonds at the interface.<sup>23</sup>

Our results also suggest that molecules containing two carboxylic acid groups (adipic, oxalic acids) are more effective at reducing the surface energy than molecules containing only one carboxylic acid group (valeric, acetic acids). Since the dicarboxylic acids also have larger adsorption coefficients, this suggests that adipic and oxalic acids likely bind to the surface using both acidic groups. The model described above does not consider the electrostatic contribution to  $K_{\text{ads}}$ . This contribution is characterized by a surface potential, which is determined by ions located within the double layer or bound to the surface. However, regardless of whether the surface potential decreases, increases, or remains constant with change in  $\Gamma$ , we infer that adsorption is greater on smaller particles. Our model result for the lowering of interfacial tension of anatase ranges from approximately  $0.2$  to  $0.6 \text{ J m}^{-2}$ , which is comparable to the heats of immersion of rutile in water ( $0.55 \text{ J m}^{-2}$ ), acetic alcohol ( $0.40 \text{ J m}^{-2}$ ), *n*-butylamine ( $0.33 \text{ J m}^{-2}$ ), and  $\text{CCl}_4$  ( $0.24 \text{ J m}^{-2}$ ).<sup>23</sup> This demonstrates the correct order of magnitude of decrease in interfacial tension due to adsorption and suggests that our presented model makes reasonable first-order predictions as to the effect of particle size on adsorption of ions onto surfaces.

For comparison, the interfacial tension of anatase after adsorption can also be calculated according to the conventional thermodynamic consideration (eq 4). The  $\gamma_{\text{O(S-L)}}$  value thus obtained is  $0.63 \text{ J m}^{-2}$  for valeric acid,  $0.76 \text{ J m}^{-2}$  for acetic acid,  $0.18 \text{ J m}^{-2}$  for adipic acid, and  $0.39 \text{ J m}^{-2}$  for oxalic acid. These values are lower than those calculated from eq 21, which means in order to reach the same equilibrium stable state after adsorption, the energy of the system must be released more according to eq 4 than according to eq 21. The following example will show that such a release according to eq 4 may lead to a physically unrealistic value of the interfacial tension.

According to ref 24, at pH 2, large-size silica ( $5 \text{ m}^2 \text{ g}^{-1}$ ) adsorbed ca. 10% Fe(III) when the total [Fe(III)] is  $1.2 \times 10^{-4} \text{ M}$ , or the adsorption of Fe(III) is  $0.009 \text{ mg m}^{-2}$  silica at an equilibrium [Fe(III)] of  $1.1 \times 10^{-4} \text{ M}$ . On the other hand, adsorption of Fe(III) on 20 nm diameter silica ( $138 \text{ m}^2 \text{ g}^{-1}$ ) at pH 2 showed a Langmuir-type adsorption, and the adsorption of Fe(III) is  $1.3 \text{ mg Fe(III) m}^{-2}$  silica at the same equilibrium concentration.<sup>25</sup> The ratio of the two adsorption quantities,  $1.3/0.009 = 144$ , can be viewed as the ratio of the two corresponding adsorption constants in accord with eq 1, given that the equilibrium concentration of Fe(III) is very low and that the maximum adsorption is assumed to be the same. By use of  $V_{\text{m}} = (60.08 \times 10^{-6})/2.17 = 2.77 \times 10^{-5} \text{ m}^3 \text{ mol}^{-1}$  for silica,<sup>25</sup>  $\gamma_{\text{O(S)}}$  =  $1.0 \text{ J m}^{-2}$  and  $\delta = 0.35 \text{ nm}$ , to make  $K_{\text{ads}}(20 \text{ nm})/K_{\text{ads}}(\text{large size}) = 144$ , the calculated  $\gamma_{\text{O(S-L)}}$  from eq 21 is  $0.06 \text{ J m}^{-2}$ , while the calculated  $\gamma_{\text{O(S-L)}}$  from eq 4 is  $-0.48 \text{ J m}^{-2}$ , which bears no physical meaning. This example illustrates that the improved thermodynamic analysis (eq 21) is more reasonable.

The extent to which the increased adsorption onto 6 nm diameter anatase particles can be attributed to changes in overall shape, resulting in an increased contribution of facets having

higher surface energy, can be estimated. Because the ratios of the average lengths measured along  $\langle 101 \rangle$  and  $\langle 001 \rangle$  by XRD are very similar for both 6 and 16 nm particles, the relative contributions to the total surface area by the  $\{101\}$  and  $\{001\}$  faces are calculated to be similar. The surface area of kinks was estimated by considering them as microfacets of fixed width. The TEM results indicate that the  $\{112\}$  and  $\{100\}$  facets, which are formed at the junctions between the dominant  $\{101\}$  and  $\{001\}$  planes, constitute less than 10% (for 6 nm particles) and 5% (for 16 nm particles) of the total surface area. Because, as a first-order approximation, surface energy varies roughly with interplanar spacing and because the extent of adsorption is approximately proportional to the reduction in surface energy, we estimate that the higher abundance of high-energy sites likely accounts for no more than 10% excess adsorption observed onto the 6 nm compared to 16 nm particles. Consequently, we can conclude that the major factor driving the higher adsorption with decrease in crystal size is the increased molar surface free energy the surface phase possesses. The enhanced chemical adsorption of several gases by nanoscale  $\text{MgO}^3$  can also be explained with a similar thermodynamic argument.

In nature, nanocrystalline products exist widely. For instance, nanocrystalline oxyhydroxide can be produced by chemical weathering reactions. Since the size effect on adsorption is significant for nanocrystalline particles, it is expected the size effect plays an important role in reactions where inorganic and organic ions are adsorbed from solutions to natural mineral surfaces or the surfaces of nanocrystalline materials. For instance, nanocrystalline oxyhydroxide products should adsorb a considerably larger proportion of ions from solution than would be predicted by simple scaling as proportional to surface area.<sup>26</sup>

## Conclusions

Thermodynamic analysis reveals that surface or interfacial tension decreases with decreasing particle size as a result of the increase in the potential energy of the bulk atoms of the particles. Smaller particles with increased molar free energy are more prone to adsorb molecules or ions per unit area onto their surfaces in order to decrease the total free energy and to become more stable, and hence, adsorption onto smaller particles has a higher adsorption coefficient. Experimental results of adsorption of organic acids onto nanocrystalline titania particles explicitly demonstrated the particle size effect on adsorption and clearly validates our thermodynamic analysis and predication.

**Acknowledgment.** Dr. Dan Sykes provided invaluable assistance with HPLC measurements. Support was provided by NSF EAR-9508171 to J.F.B. and a National Physical Science Consortium Fellowship (sponsored by Sandia National Laboratories) to R.L.P.

## References and Notes

- (1) Sverjensky, D. A. *Nature (London)* **1993**, 364, 776.
- (2) Alivisatos, A. P. *Science* **1996**, 271, 933.
- (3) (a) Stark, J. V.; Park, D. G.; Lagadic, I.; Klabunde, K. J. *Chem. Mater.* **1996**, 8, 1904. (b) Stark, J. V.; Klabunde, K. J. *Chem. Mater.* **1996**, 8, 1913.
- (4) Atteya, M.; Klabunde, K. J. *Chem. Mater.* **1991**, 3, 182.
- (5) Vayssieres, L.; Chaneac, C.; Tronc, E.; Jolivet, J. P. *J. Colloid Interface Sci.* **1998**, 205, 205.
- (6) Furusawa, K.; Shou, Z.; Nagahashi, N. *Colloid Polym. Sci.* **1992**, 270, 212.
- (7) Katari, J. E.; Colvin, V. L.; Alivisatos, A. P. *J. Phys. Chem.* **1994**, 98, 4109.
- (8) Luzinov, I.; Evchuk, I.; Minko, S.; Voronov, S. *J. Appl. Polym. Sci.* **1998**, 67, 299.

- (9) Langmuir, I. *J. Am. Chem. Soc.* **1916**, 38, 2221.
- (10) Terwilliger, C. D.; Chiang, Y. M. *J. Am. Ceram. Soc.* **1995**, 78, 2045.
- (11) Li, X. P.; Shih, W. H. *J. Am. Ceram. Soc.* **1997**, 80, 2844.
- (12) Sun, N. X.; Lu, K.; Jiang, Q. *Phys. Rev. B* **1997**, 56, 5885.
- (13) Tolman, R. C. *J. Chem. Phys.* **1949**, 17, 333.
- (14) Moore, W. J. *Physical Chemistry*, 4th ed.; Prentice-Hall: Englewood Cliffs, NJ, 1972; pp 97–99.
- (15) Blakely, J. M. *Introduction to the Properties of Crystal Surfaces*; Pergamon Press: New York, 1973; pp 7–10.
- (16) Cammarata, R. C.; Sieradzki, K. *Annu. Rev. Mater. Sci.* **1994**, 24, 215.
- (17) Zhang, H.; Banfield, J. F. *J. Mater. Chem.* **1998**, 8, 2073.
- (18) Gribb, A. A.; Banfield, J. F. *Am. Mineral.* **1997**, 82, 717.
- (19) Bischoff, B. L. Ph.D. Thesis, University of Wisconsin–Madison, WI, 1992.
- (20) (a) Penn, R. L.; Banfield, J. F. *Geochim. Cosmochim. Acta*, in press.  
(b) Penn, R. L.; Banfield, J. F. *Am. Mineral.* **1998**, 83, 1077.
- (21) Weast, R. C.; Astle, M. J.; Beyer, W. H. *CRC Handbook of Chemistry and Physics*, 66th ed.; CRC Press: Boca Raton, FL, 1985; p B-154.
- (22) The value for  $\gamma_o(\text{anatase})$  from ref 17, 1.32 J/m<sup>2</sup>, is used to estimate the interfacial tension of anatase in water. According to Fowkes,<sup>27</sup> the equilibrium spreading pressure of an adsorbed water film on anatase is  $\pi_e = 0.30$  J/m<sup>2</sup>. Hence,  $\gamma_o(\text{anatase-H}_2\text{O}) = \gamma_o(\text{anatase}) - \pi_e - \gamma_o(\text{H}_2\text{O}) = 1.32 - 0.3 - 0.07 = 0.95$  J/m<sup>2</sup>. So, we assume  $\gamma_{o(s)} = 1.0$  J/m<sup>2</sup>.
- (23) Adamson, A. W. *Physical Chemistry of Surfaces*, 5th ed.; John Wiley & Sons: New York, 1990; pp 88–96, 382.
- (24) James, R. O.; Healy, T. W. *J. Colloid Interface Sci.* **1972**, 40, 42.
- (25) Maeda, S.; Armes, S. P. *J. Mater. Chem.* **1994**, 4, 935.
- (26) Banfield, J. F.; Hamers, R. J. In *Geomicrobiology: Interactions between Microbes and Minerals, Reviews in Mineralogy*; Banfield, J. F., Nealon, K. H., Eds.; Mineralogical Society of America: Washington, DC, 1997; pp 81–122.
- (27) Fowkes, F. M. In *Chemistry and Physics of Interfaces*; American Chemical Society: Washington, DC, 1965; pp 1–12.